

OVERVIEW AND SUMMARY

This report is the fourth in a series of periodic reports that describe the data collected by the Interagency Monitoring of Protected Visual Environments (IMPROVE) monitoring network. The IMPROVE program is a cooperative measurement effort between the U.S. Environmental Protection Agency (EPA), federal land management agencies, and state air agencies designed to

1. establish current visibility and aerosol conditions in mandatory Class I areas (CIAs);
2. identify chemical species and emission sources responsible for existing man-made visibility impairment;
3. document long-term trends for assessing progress towards the national visibility goal;
4. and, with the enactment of the Regional Haze Rule, provide regional haze monitoring representing all visibility-protected federal CIAs where practical.

When the IMPROVE monitoring program was initiated, it was resource and funding limited so that it was not practical to place monitoring stations at all 156 mandatory Class I areas where visibility is an important attribute. Therefore, the first IMPROVE report reflected data that were collected at only 36 sites for the time period March 1988 through February 1991. Over subsequent years the IMPROVE network evolved and a second IMPROVE report was published that covered data gathered between March 1992 and February 1995 at 43 sites. The network is now composed of 110 IMPROVE sites representative of 155 of the 156 visibility-protected federal Class I areas (national parks and wilderness areas). There are an additional ~50 IMPROVE protocol sites operated identically to the 110 IMPROVE sites but which are individually sponsored by federal, state, and tribal organizations (see Figure S.1).

This report provides a broad examination of the IMPROVE data as well as results from special field studies and data analyses conducted since the 2000 IMPROVE report. The IMPROVE data analysis includes the examination of the spatial and seasonal aerosol concentrations and composition for 159 sites from 2000 through 2004 and long-term trends for 38–49 sites, depending upon the parameter examined, using data from 1988 and 2004. A unique aspect of this report compared to previous IMPROVE reports is the inclusion of 84 sites from the EPA's Speciated Trend Network (STN) in the spatial and seasonal pattern analyses. The STN network collects speciated aerosol data similar to the IMPROVE network, but the sites are located primarily in urban/suburban settings. Incorporation of data from these sites into the assessment permits the extension of the spatial and season aerosol patterns from the surrounding remote areas into urban areas, providing insights into the fraction of the particulate matter (PM) that is contributed by regional and local sources.

IMPROVE quality assurance (QA) procedures are continually reviewed and enhanced. During the recent network expansion (2000 to 2002), collocated monitors were installed at a number of IMPROVE sites to provide data needed to assess measurement precision. This report summarizes the current QA procedures and the results of precision estimates from collocated monitors.

S.1 OPTICAL AND AEROSOL DATA

The IMPROVE aerosol samplers (versions I and II) consist of four independent modules. Each module incorporates a separate inlet, filter pack, and pump assembly. It is convenient to consider a particular module, its associated filter, and the parameters measured from the filter as a channel of measurement (e.g., module A). Modules A, B, and C are equipped with a 2.5 µm cyclone, while module D is fitted with a PM₁₀ inlet. The D module collects PM₁₀ aerosol on Teflon filters. The A, B, and C modules collect PM_{2.5} aerosol on Teflon, nylon, and quartz fiber filters, respectively. The different filter media facilitate the collection of particular aerosol species or a specific form of chemical analysis. Gravimetric analysis is routinely performed on the A and D module filters. Elemental analysis and aerosol absorption measurements are routinely performed on the A module filter. Ion analysis is routinely performed on the B module filter, and carbon analysis is routinely performed on the quartz fiber filter. The samplers are currently operated on a one-day-in-three schedule for a 24-hour sampling duration consistent with the EPA's aerosol monitoring networks. There are aerosol samplers at the 110 IMPROVE sites and the ~50 IMPROVE protocol sites. Current and past IMPROVE and protocol aerosol sampling sites are listed by region in Table S.1, and those in the contiguous 48 states are shown in Figure S.1.

Table S.1. IMPROVE monitoring sites listed according to region. The monitoring site codes are in parentheses.

Alaska	Northeast
• Ambler (AMBL1)*	• Acadia NP (ACAD1)
• Denali NP (DENA1)	• Addison Pinnacle (ADPI1)
• Petersburg (PETE1)	• Bridgton (BRMA1)
• Simeonof (SIME1)	• Cape Cod (CACO1)
• Trapper Creek (TRCR1)	• Casco Bay (CABA1)
• Tuxedni (TUXE1)	• Connecticut Hill (COHI1)*
Appalachia	• Great Gulf WA (GRGU1)
• Arendtsville (AREN1)	• Lye Brook WA (LYBR1)
• Cohutta (COHU1)	• Martha's Vineyard (MAVI1)
• Dolly Sods WA (DOSO1)	• Mohawk Mt. (MOMO1)
• Frostburg (FRRE1)	• Moosehorn NWR (MOOS1)
• Great Smoky Mountains NP (GRSM1)	• Old Town (OLTO1)
• James River Face WA (JARI1)	• Presque Isle (PRIS1)
• Jefferson NF (JEFF1)*	• Proctor Maple R. F. (PMRF1)
• Linville Gorge (LIGO1)	• Quabbin Summit (QURE1)
• Shenandoah NP (SHEN1)	Northern Great Plains
• Shining Rock WA (SHRO1)	• Badlands NP (BADL1)
• Sipsy WA (SIPS1)	• Cloud Peak (CLPE1)
Boundary Waters	• Fort Peck (FOPE1)
• Boundary Waters Canoe Area (BOWA1)	• Lostwood (LOST1)
• Isle Royale NP (ISLE1)	• Medicine Lake (MELA1)
• Isle Royale NP (ISRO1)*	• Northern Cheyenne (NOCH1)
• Seney (SENE1)	• Theodore Roosevelt (THRO1)
• Voyageurs NP #1 (VOYA1)*	• Thunder Basin (THBA1)
• Voyageurs NP #2 (VOYA2)	• UL Bend (ULBE1)
California Coast	• Wind Cave (WICA1)
• Pinnacles NM (PINN1)	Northern Rockies
• Point Reyes National Seashore (PORE1)	• Bridger WA (BRID1)
• San Rafael (RAFA1)	• Cabinet Mountains (CABI1)

Central Great Plains	• Flathead (FLAT1)
• Blue Mounds (BLMO1)	• Gates of the Mountains (GAMO1)
• Bondville (BOND1)	• Glacier NP (GLAC1)
• Cedar Bluff (CEBL1)	• Monture (MONT1)
• Crescent Lake (CRES1)	• North Absaroka (NOAB1)
• El Dorado Springs (ELDO1)	• Salmon NF (SALM1)*
• Great River Bluffs (GRRI1)	• Sula Peak (SULA1)
• Lake Sugema (LASU1)*	• Yellowstone NP 1 (YELL1)
• Lake Sugema (LASU2)	• Yellowstone NP 2 (YELL2)
• Nebraska NF (NEBR1)	Northwest
• Omaha (OMAH1)	• Lynden (LYND1)*
• Sac and Fox (SAFO1)	• Mount Rainier NP (MORA1)
• Tallgrass (TALL1)	• North Cascades (NOCA1)
• Viking Lake (VILA1)	• Olympic (OLYM1)
Central Rockies	• Pasayten (PASA1)
• Brooklyn Lake (BRLA1)*	• Snoqualmie Pass (SNPA1)
• Great Sand Dunes NM (GRSA1)	• Spokane Res. (SPOK1)*
• Mount Zirkel WA (MOZI1)	• White Pass (WHPA1)
• Rocky Mountain NP (ROMO1)	Not Assigned
• Rocky Mountain NP HQ (RMHQ1)*	• Walker River Paiute Tribe (WARI1)*
• Storm Peak (STPE1)*	Ohio River Valley
• Wheeler Peak (WHPE1)	• Cadiz (CAD11)
• White River NF (WHR11)	• Livonia (LIVO1)
Colorado Plateau	• M.K. Goddard (MKGO1)
• Arches NP (ARCH1)*	• Mammoth Cave NP (MACA1)
• Bandelier NM (BAND1)	• Mingo (MING1)
• Bryce Canyon NP (BRCA1)	• Quaker City (QUCI1)
• Canyonlands NP (CANY1)	Oregon and Northern California
• Capitol Reef NP (CAPI1)	• Bliss SP (TRPA) (BLIS1)
• Hance Camp at Grand Canyon NP (GRCA2)	• Crater Lake NP (CRLA1)
• Hopi Point #1 (GRCA1)*	• Kalmiopsis (KALM1)
• Indian Gardens (INGA1)	• Lassen Volcanic NP (LAVO1)
• Meadview (MEAD1)	• Lava Beds NM (LABE1)
• Mesa Verde NP (MEVE1)	• Mount Hood (MOHO1)
• San Pedro Parks (SAPE1)	Phoenix
• Weminuche WA (WEMI1)	• Phoenix (PHOE1)
• Zion (ZION1)*	Puget Sound
• Zion Canyon (ZICA1)	• Puget Sound (PUSO1)
Columbia River Gorge	• Redwood NP (REDW1)
• Columbia Gorge #1 (COGO1)	• Three Sisters WA (THSI1)
• Columbia River Gorge (CORI1)	• Trinity (TRIN1)
Death Valley	Sierra Nevadas
• Death Valley NP (DEVA1)	• Dome Lands WA (DOLA1)*
East Coast	• Dome Lands WA (DOME1)
• Brigantine NWR (BRIG1)	• Hoover (HOOV1)
• Swanquarter (SWAN1)	• Kaiser (KAIS1)
Great Basin	• Sequoia NP (SEQU1)
• Great Basin NP (GRBA1)	• South Lake Tahoe (SOLA1)*
• Jarbidge WA (JARB1)	• Yosemite NP (YOSE1)
Hawaii	Southeast
• Haleakala NP (HALE1)	• Breton (BRET1)
• Hawaii Volcanoes NP (HAVO1)	• Cape Romain NWR (ROMA1)
• Mauna Loa Observatory #1 (MALO1)	• Chassahowitzka NWR (CHAS1)
	• Everglades NP (EVER1)

• Mauna Loa Observatory #2 (MALO2)	• Okefenokee NWR (OKEF1)
• Mauna Loa Observatory #3 (MALO3)*	• St. Marks (SAMA1)
• Mauna Loa Observatory #4 (MALO4)*	Southern Arizona
Hells Canyon	• Chiricahua NM (CHIR1)
• Craters of the Moon NM (CRMO1)	• Douglas (DOUG1)
• Hells Canyon (HECA1)	• Organ Pipe (ORPI1)
• Sawtooth NF (SAWT1)	• Queen Valley (QUVA1)
• Scoville (SCOV1)*	• Saguaro NM (SAGU1)
• Starkey (STAR1)	• Saguaro West (SAWE1)
Lone Peak	Southern California
• Lone Peak WA (LOPE1)*	• Agua Tibia (AGTI1)
Mid South	• Joshua Tree NP (JOSH1)
• Caney Creek (CACR1)	• Joshua Tree NP (JOTR1)*
• Cherokee Nation (CHER1)	• San Gabriel (SAGA1)
• Ellis (ELLI1)	• San Gorgonio (SAGO5)
• Hercules-Glades (HEGL1)	• San Gorgonio WA (SAGO1)
• Sikes (SIKE1)	Urban QA Sites
• Upper Buffalo WA (UPBU1)	• Atlanta (ATLA1)
• Wichita Mountains (WIMO1)	• Baltimore (BALT1)
Mogollon Plateau	• Birmingham (BIRM1)
• Bosque del Apache (BOAP1)	• Chicago (CHIC1)
• Gila WA (GICL1)	• Detroit (DETR1)
• Hillside (HILL1)*	• Fresno (FRES1)
• Ike's Backbone (IKBA1)	• Houston (HOUS1)
• Mount Baldy (BALD1)	• New York City (NEYO1)
• Petrified Forest NP (PEFO1)	• Pittsburgh (PITT1)
• San Andres (SAAN1)*	• Rubidoux (RUBI1)*
• Sierra Ancha (SIAN1)	Virgin Islands
• Sierra Ancha (SIAN1)	• Virgin Islands NP (VIIS1)
• Sycamore Canyon (SYCA1)	Washington D.C.
• Tonto NM (TONT1)	• Washington D.C. (WASH1)
• White Mountain (WHIT1)	West Texas
	• Big Bend NP (BIBE1)
	• Guadalupe Mountains NP (GUMO1)
	• Salt Creek (SACR1)

NF = National Forest

NM = National Monument

NP = National Park

NWR = National Wildlife Refuge

WA = Wilderness Area

*Discontinued sites

IMPROVE Aerosol Network

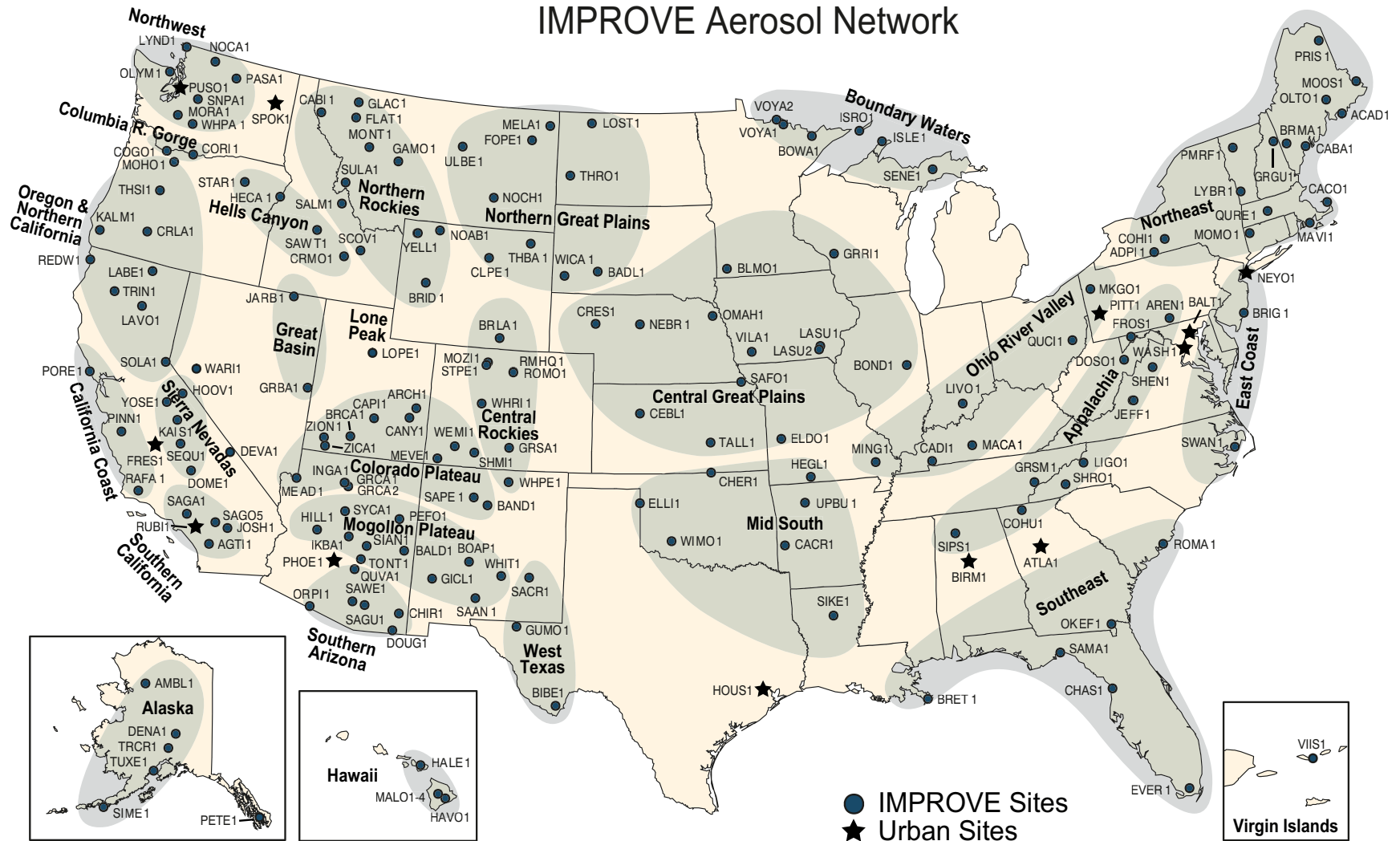


Figure S.1. The locations current and discontinued IMPROVE and IMPROVE protocol monitoring sites as of December 2004. The IMPROVE regions used for grouping the sites in some analyses in this report are indicated by green shading and bold text. Urban sites included in the IMPROVE network for quality assurance purposes are identified by stars.

S.2 SPATIAL TRENDS IN AEROSOL CONCENTRATION AND EXTINCTION

The spatial trends in $PM_{2.5}$ and b_{ext} and their constituents were examined using 2000–2004 data from the integrated IMPROVE and STN data set. PM_{10} is not measured in the STN network, so only coarse mass from the IMPROVE network was examined, and b_{ext} could only be estimated for IMPROVE sites. Appendix E assesses the comparability of data from collocated IMPROVE and STN sites to determine the appropriateness of combining the data from these two networks. It was found that on average the annual STN $PM_{2.5}$, sulfate, nitrate and organics concentrations between the STN and IMPROVE were within 2% of the IMPROVE concentrations. However, the STN fine soil and light-absorbing carbon (LAC) were respectively 30% and 10% lower than that measured by IMPROVE.

The major aerosol species are calculated by scaling measured elemental and ionic concentrations to assumed forms of particulate matter, e.g., ammonium sulfate. The particulate light extinction is calculated from these aerosol species concentrations by multiplying the concentration of a given species by its light-extinction efficiency and summing over all species. Sulfates and nitrates are hygroscopic, so their light-extinction efficiencies increase with relative humidity and are adjusted using a nonlinear relative humidity factor based on monthly averaged relative humidity at each site.

Haziness is characterized by an index with deciview (dv) units, which are related to the logarithm of the sum of the particulate b_{ext} and Rayleigh scattering. A change of 1 dv is usually perceived as a small change in haziness, regardless of the initial haze level. The spatial deciview and reconstructed b_{ext} maps are presented in Figures S.2 and S.3. Because higher b_{ext} leads to higher dv, the geographic trends in visibility (dv) are similar to the trends in reconstructed extinction. In addition, the deciview and reconstructed b_{ext} varies throughout the United States in a way analogous to fine aerosol concentrations.

The greatest particulate b_{ext} occurred in the eastern United States and in southern California, while the smallest values occurred in the nonurban West (e.g., the Great Basin and the Colorado Plateau) and in Alaska. The difference between eastern and western light extinction is even more pronounced than the difference in aerosol concentrations, because relative humidity, and therefore the light-scattering efficiency of sulfate and nitrate, is higher in the East than in the West. The smallest dv values, or best visibility, are in Alaska and a broad region including the Great Basin, most of the Colorado Plateau, and portions of the central Rockies, which have visibility impairment of less than 10 dv. Moving in any direction from this region generally results in increasing dv values. West of the Sierra Nevada and including southern California, one finds dv values greater than 14, with a maximum value of 18.9 dv at Sequoia National Park. The northwest United States and the entire eastern half of the United States have in excess of 14 dv of impaired visibility. The regions east of the Mississippi and south of the Great Lakes have impairment in excess of 20 dv. The highest annual dv was about 24, occurring in the general region of the Ohio River and Tennessee valleys.

Fine aerosols are the most effective in scattering light and are the major contributor to light extinction. Ammonium sulfate is among the most important contributors to b_{ext} . In the eastern United States, sulfate accounted for 45–60% of the reconstructed fine mass in rural locations. The contribution was smaller in the western United States and urban locations,

varying from 15% to 40% of the reconstructed fine mass. The highest ammonium sulfate concentrations were found in the Ohio River valley, where there are significant SO₂ emissions, and the Appalachian Mountains at 6–8 µg/m³. Ammonium sulfate concentrations were less than 1 µg/m³ in most of the western United States. The urban STN sites had similar ammonium sulfate concentrations to nearby rural sites and rarely exceed 2 times the nearby rural concentrations.

The spatial patterns in extinction and mass concentration attributed to ammonium sulfate were very similar but with steeper gradients observed in extinction (Figures S.4 and S.5). For example, the central eastern United States concentrations are about a factor of 8 larger than those in the interior western United States, but the b_{ext} values are about a factor of 12 larger.

Peak rural organic mass by carbon (OMC) concentrations and OMC b_{ext} (Figure S.6) occurred in the Northwest, in the mountains of California, and in the southeastern United States. A large band through the interior West, from the Mexico border into the upper Midwest, had low rural OMC values. The urban STN sites had high OMC concentrations and light scattering in the interior West, Northeast, and Midwest relative to nearby rural sites (Figure S.7). All of the western states with both urban and rural sites had urban concentrations at least 2 times higher than nearby rural concentrations. In the eastern United States, the urban excess was generally smaller, with the largest excess occurring in the southeastern United States and along the Atlantic seaboard. In the northwestern United States, OMC accounted for more than 50% of the reconstructed fine mass and b_{ext} .

Rural LAC concentrations were low, typically less than 0.5 µg/m³. Urban LAC concentrations were higher than neighboring rural sites, with average concentrations about 1 µg/m³ or greater at urban centers throughout the United States. These concentrations represent less than 8% of the reconstructed fine mass at all locations. The contribution of LAC to b_{ext} was also small, typically less than 10%.

Rural and urban ammonium nitrate concentrations and nitrate b_{ext} were high in California and the central Great Plains and Great Lakes regions of the Midwest where both NO_x and ammonia emissions are high (Figures S.8 and S.9). The highest rural nitrate light scattering was in the Midwest at 20–27 Mm⁻¹. The highest urban extinction coefficients, between 60 and 90 Mm⁻¹, were in metropolitan Los Angeles and the San Joaquin Valley, California. In past IMPROVE reports and spatial analyses, the IMPROVE network did not contain Midwest monitoring sites, and the Midwest nitrate “bulge” was missing from these analyses. All urban sites had excess ammonium nitrate compared to neighboring rural sites. The largest excess occurred in California, the mountainous West, and the Great Lakes regions where it was 2–12 µg/m³ or 12–74 Mm⁻¹.

The spatial patterns in fine soil concentrations and light scattering were quite distinct from those for ammonium sulfate, ammonium nitrate, and OMC—it is the only fine aerosol parameter to show peak values in the arid Southwest, where in rural areas it contributes to 20–45% of the reconstructed fine mass and up to 10% of the particulate b_{ext} (Figures S.10 and S.11). For most of the United States, urban soil mass concentrations were in the same concentration range as neighboring rural sites. The exceptions include Alaska, Alabama, Nebraska, and Ohio, where the urban concentrations were over 2 times those at the rural sites in the state. In urban

areas the soil concentrations accounted for less than 20% of the reconstructed fine mass, except for Puerto Rico.

The coarse mass is typically dominated by contributions from soil. However, as shown by comparing Figures S.10 and S.12, there are large differences in the spatial patterns in fine soil and coarse mass concentrations and light scattering. The coarse mass spatial patterns have a large “bulge” in the agriculturally intensive Midwest that is not seen in the fine soil. In addition, coastal sites have high coarse mass values relative to fine soil. At the rural sites, the coarse mass has its highest contributions to light scattering in the Southwest where it contributed to 20% or more of the particulate b_{ext} .

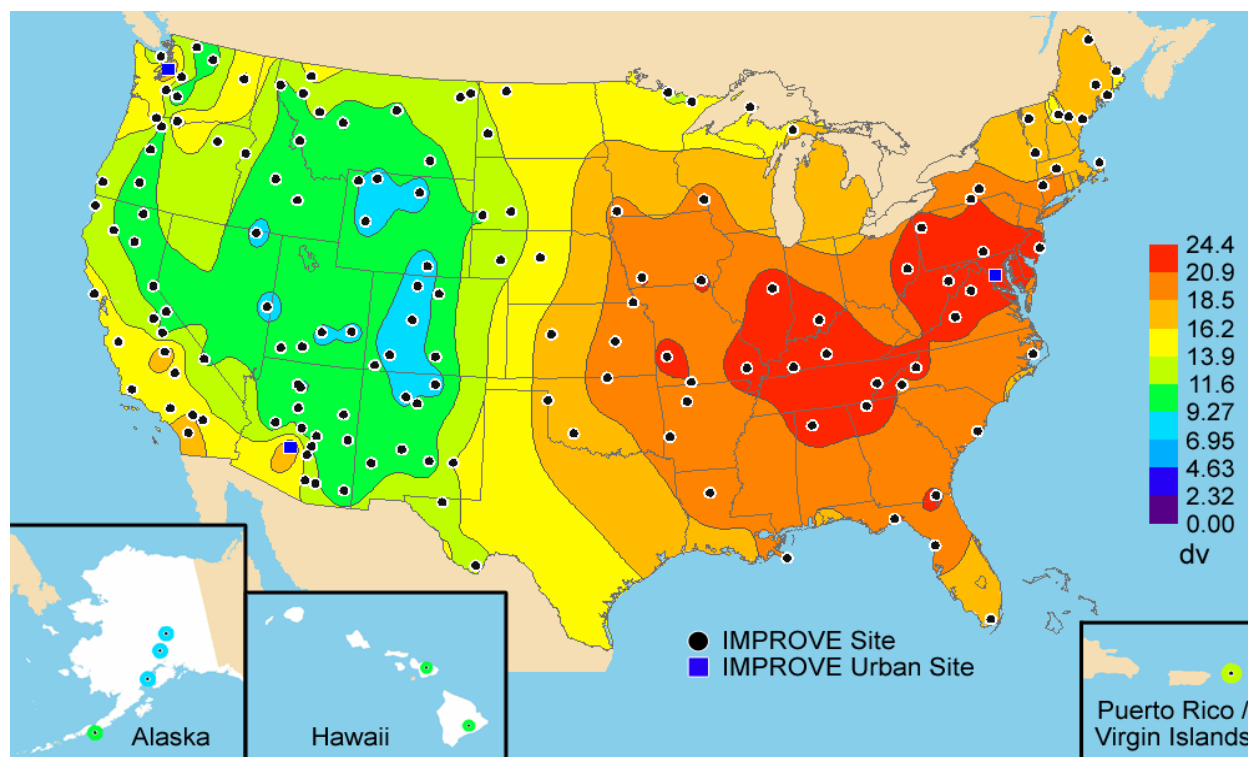


Figure S.2. Five-year average (2000–2004) deciview (DV) using only IMPROVE data.

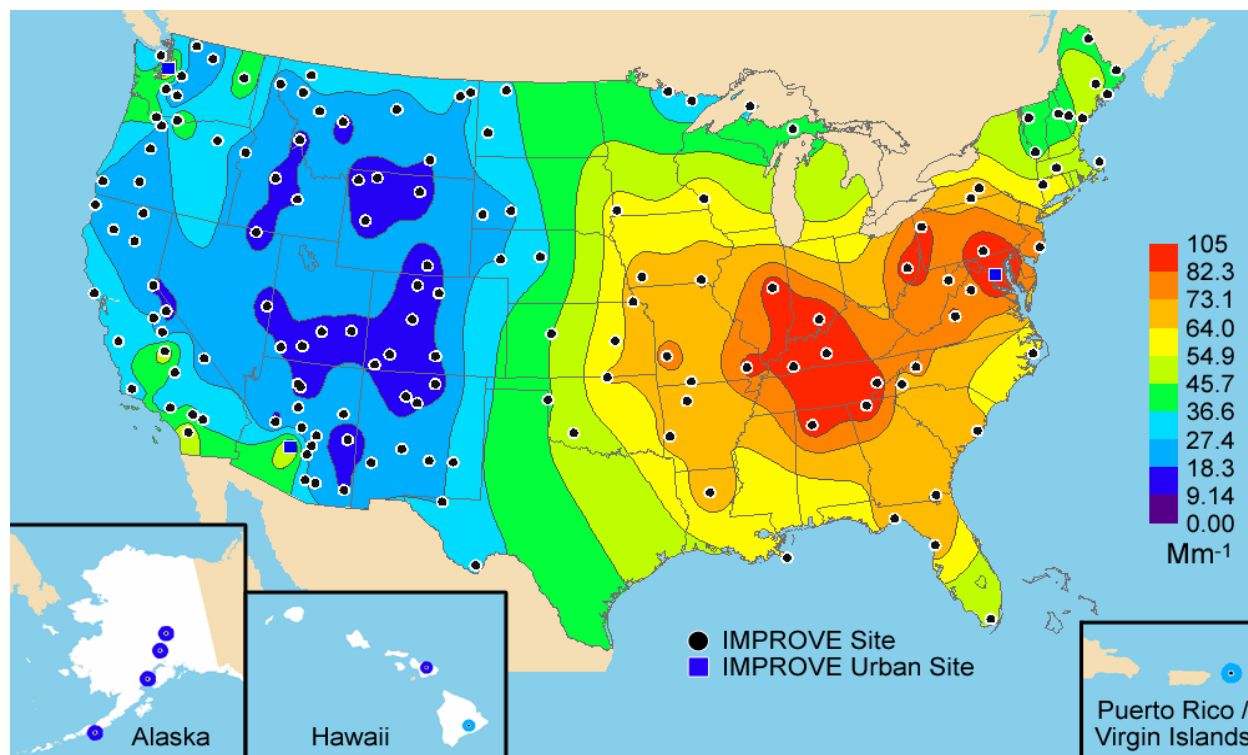


Figure S.3. Five-year average (2000–2004) reconstructed particulate light extinction using only IMPROVE data.

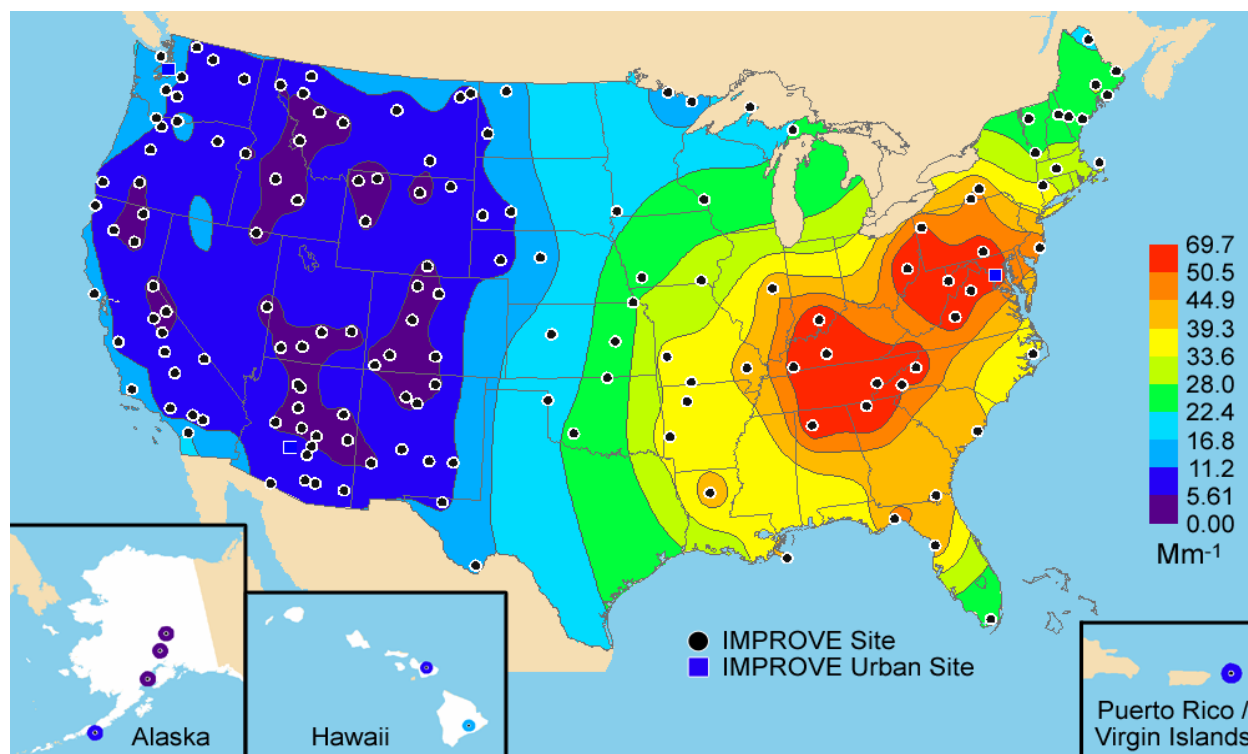


Figure S.4. Five-year average (2000–2004) sulfate light scattering using only IMPROVE data.

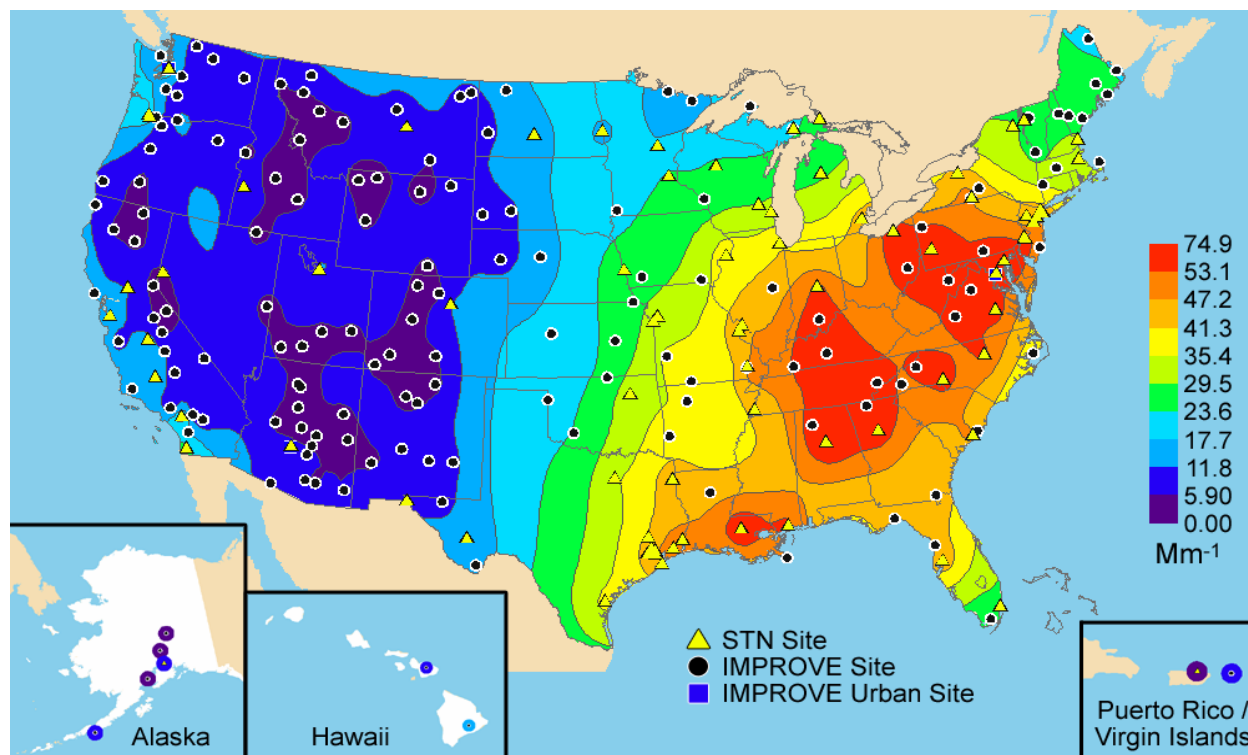


Figure S.5. Five-year average (2000–2004) sulfate light scattering using IMPROVE and STN data.

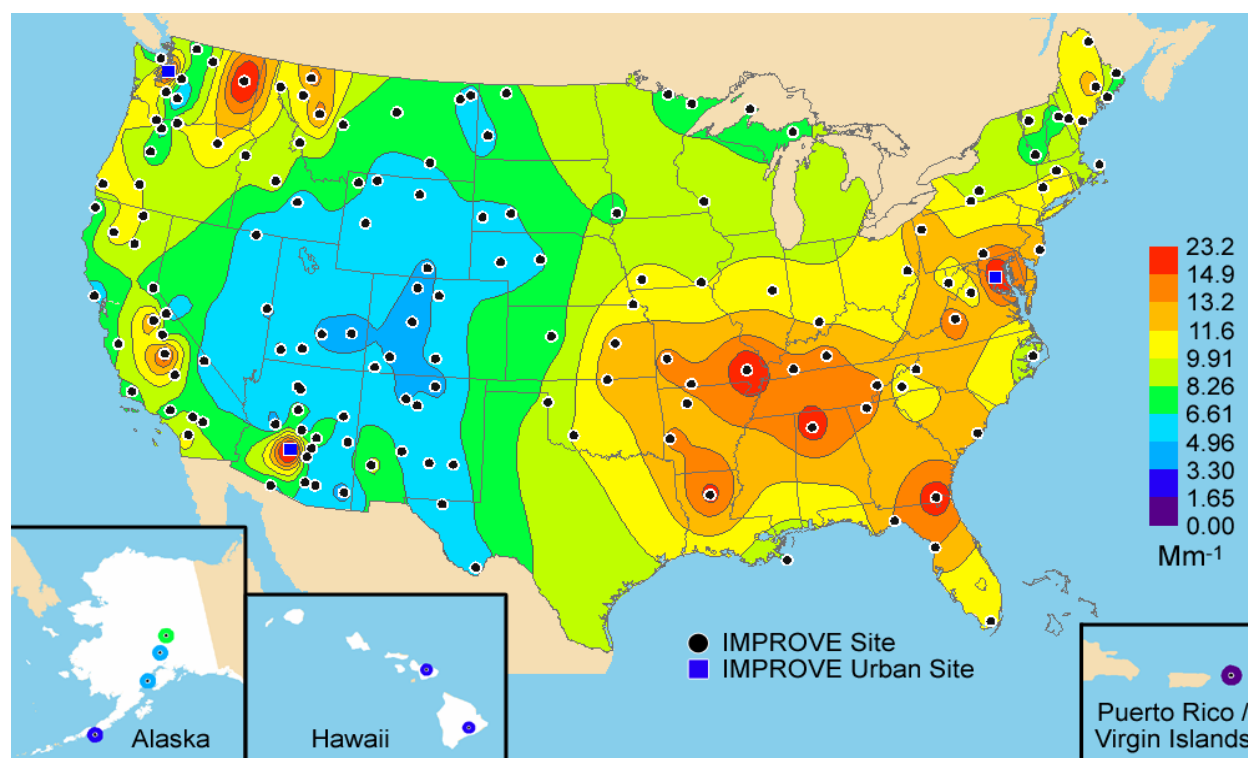


Figure S.6. Five-year average (2000–2004) organic carbon light scattering using only IMPROVE data.

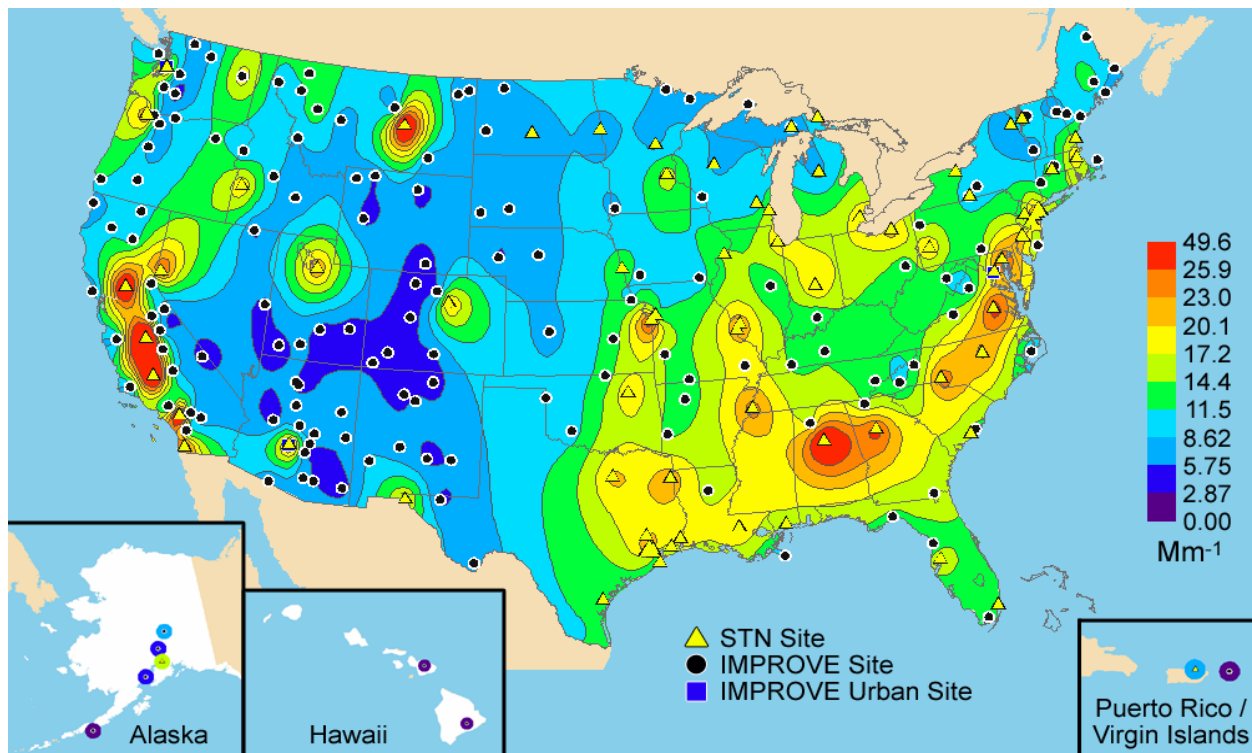


Figure S.7. Five-year average (2000–2004) organic carbon light scattering using IMPROVE and STN data.

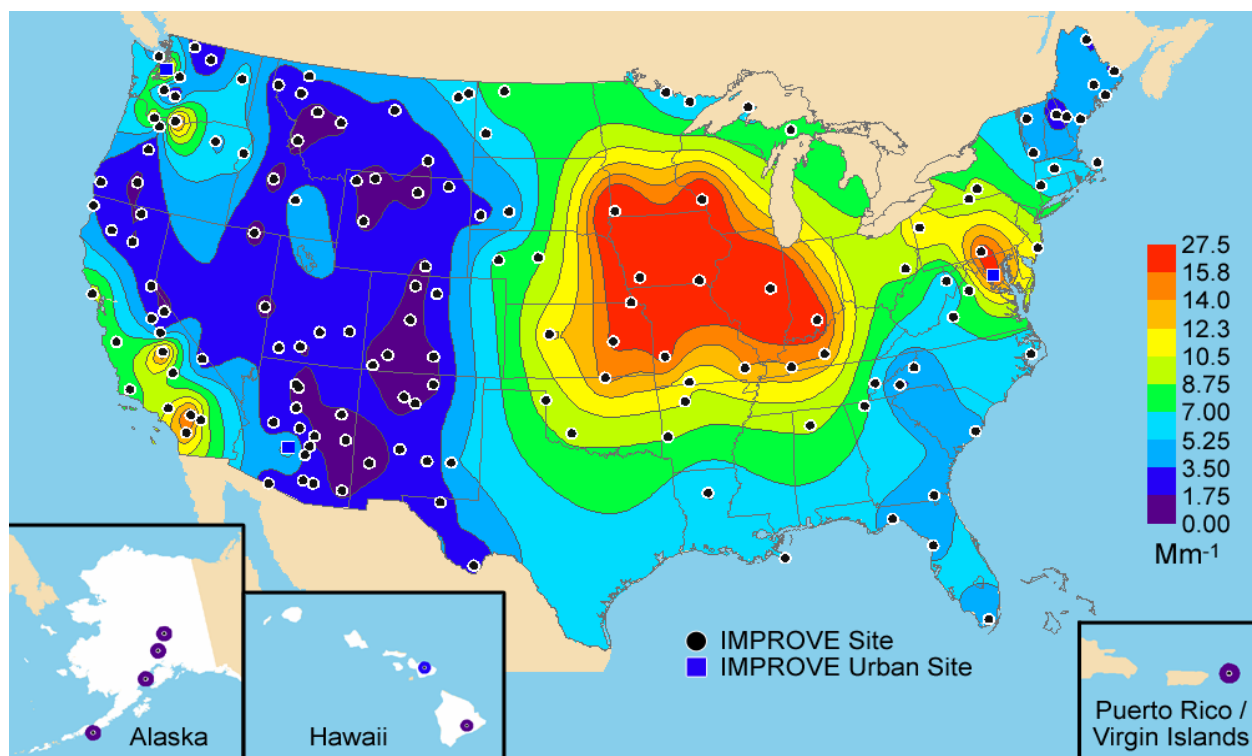


Figure S.8. Five-year average (2000–2004) ammonium nitrate light scattering using only IMPROVE data.

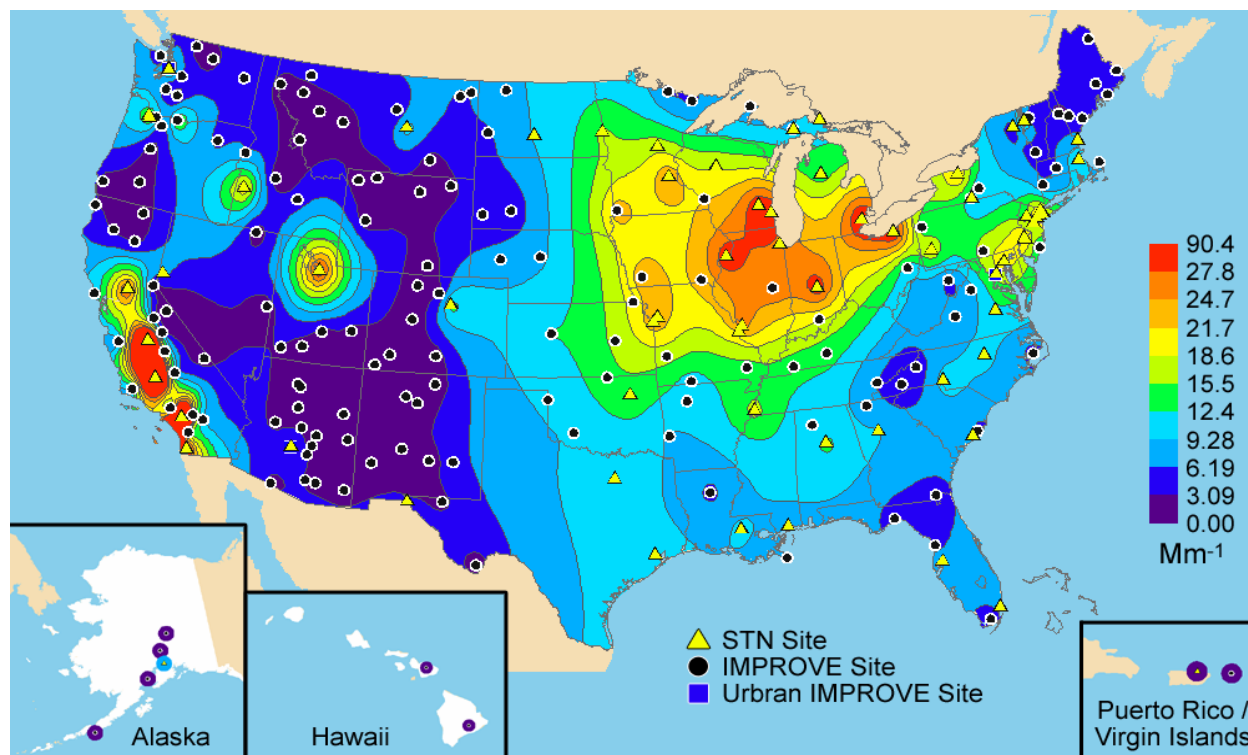


Figure S.9. Five-year average (2000–2004) ammonium nitrate light scattering using IMPROVE and STN data.

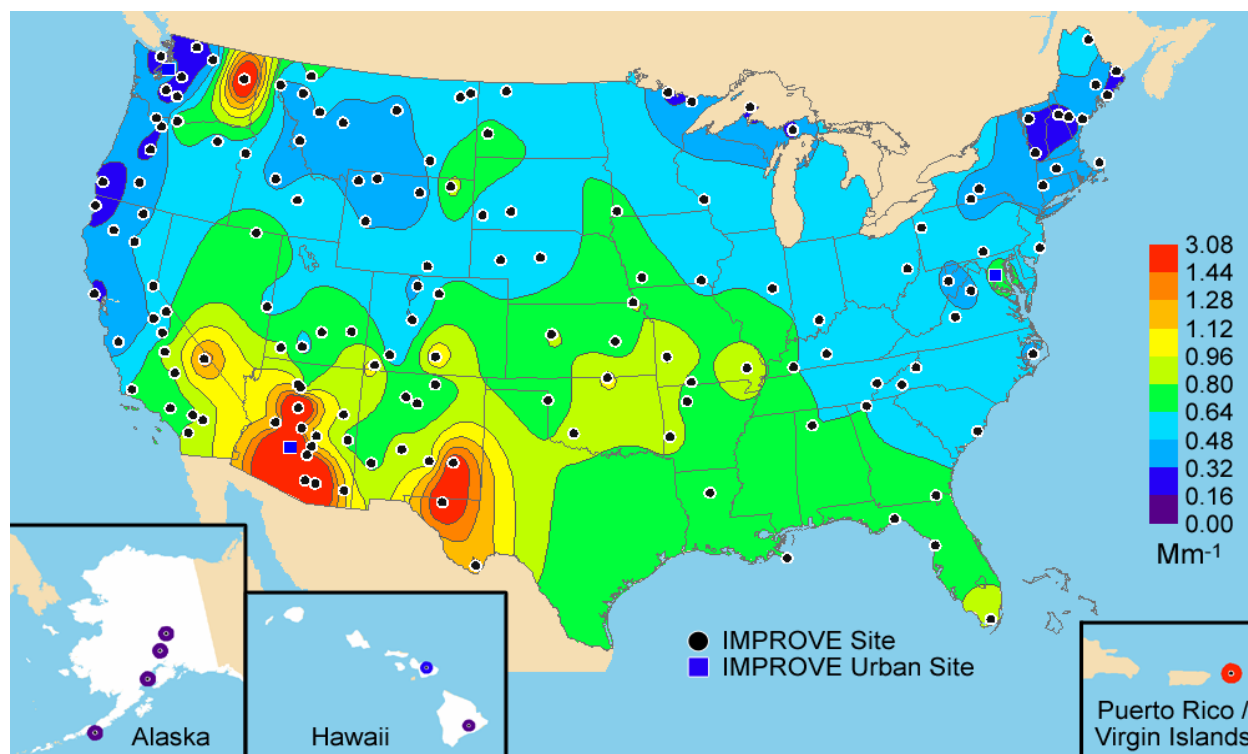


Figure S.10. Five-year average (2000–2004) fine soil light scattering using only IMPROVE data.

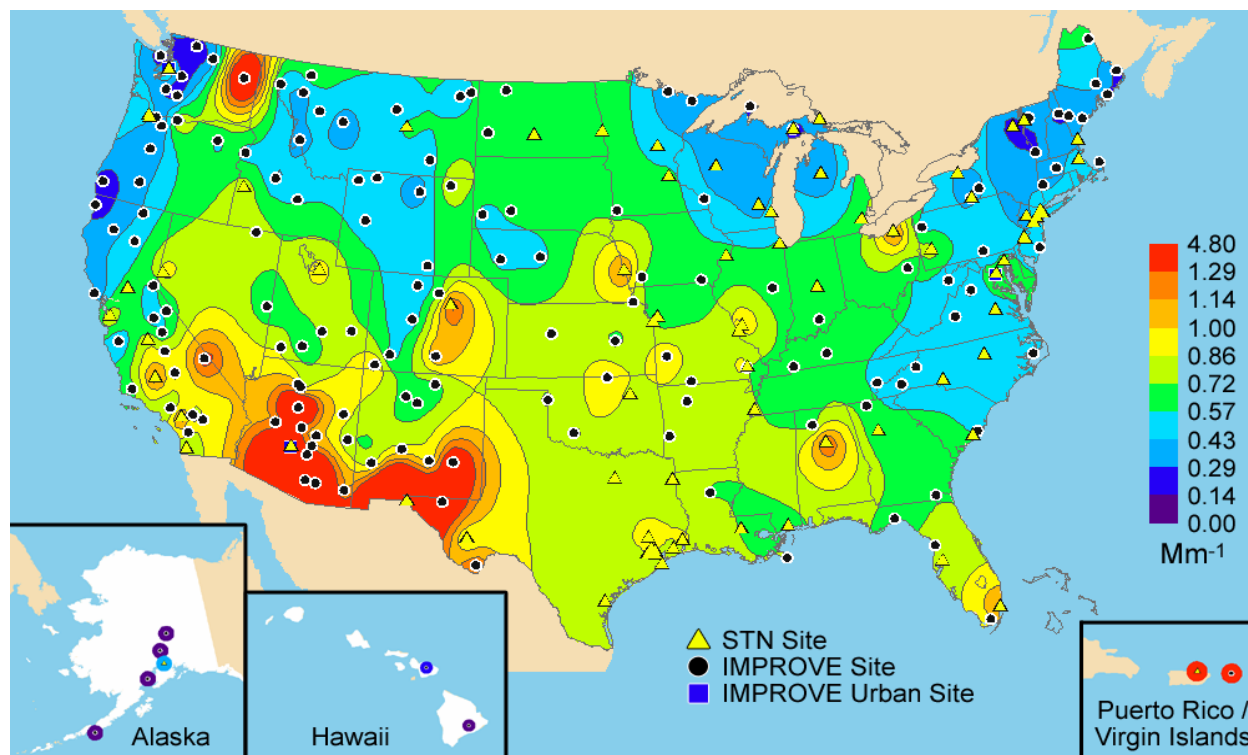


Figure S.11. Five-year average (2000–2004) fine soil light scattering using IMPROVE and STN data. Note comparisons of collocated data indicate the STN fine soil concentrations and light scattering were typically 30% smaller than from the IMPROVE monitors.

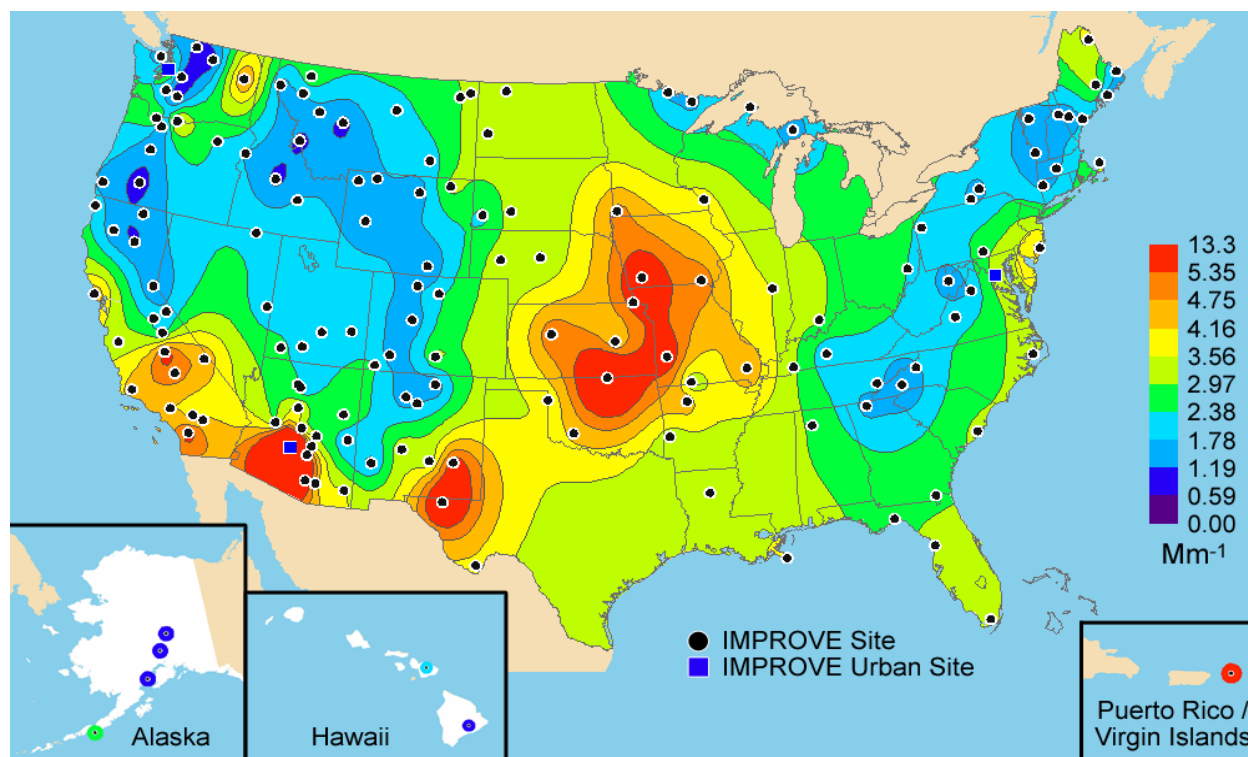


Figure S.12. Five-year average (2000–2004) coarse mass light scattering using only IMPROVE data.

S.3 SPATIAL VARIABILITY OF AVERAGE MONTHLY PATTERNS IN FINE AEROSOL SPECIES CONCENTRATIONS AND AEROSOL EXTINCTION COEFFICIENTS

The seasonal composition of the IMPROVE and STN particulate contributions to b_{ext} for various regions is summarized in Figures S.13, S.14, and S.15. Note that the STN network does not include light scattering by coarse mass. As shown in Figure S.13, in the rural eastern United States, b_{ext} peaks during the summer months, driven by the ammonium sulfate light scattering. The exception is in the central Great Plains and Boundary Waters regions where there are summer and winter peaks. The winter peaks are due to increased ammonium nitrate scattering when ammonium sulfate values are low. At the urban sites, b_{ext} has a summer and a winter peak in most regions. The summer peak is due to increased light scattering by ammonium sulfate and organics, while the winter peak is due to increased ammonium nitrate light scattering. Fine soil, coarse mass, and light absorption are small contributors to b_{ext} during all months in the eastern United States. However, at the Virgin Islands site, fine soil and coarse mass contribute about half of the b_{ext} and peak May–September.

In the rural southwestern United States (Figure S.14), the b_{ext} generally peaks in spring and summer months, when light scattering by ammonium sulfate, organics, and soil are highest. Ammonium nitrate is a small contributor to b_{ext} , except in California where the highest ammonium nitrate light scattering occurs in the colder months from November to March. In the southwestern urban regions, b_{ext} generally peaks between November and February. This b_{ext} peak is caused by increased light scattering by ammonium nitrate as well as organics. Summer peaks in organics also occurred at Denver, Colorado, and in western Nevada. Los Angeles is unique in that b_{ext} peaks during the summer months due to increased light scattering by ammonium sulfate.

In the rural northwestern United States (Figure S.15), the seasonality of b_{ext} is varied. In Alaska and the northern Rockies and northern California/Oregon regions, there are pronounced summer peaks due primarily to increased light scattering from organics compared to winter months. The Northwest region also has a summer peak in b_{ext} due to similar increases in light scattering from organics and ammonium sulfate. The Columbia River Gorge and Hells Canyon regions have winter b_{ext} peaks due to increased ammonium nitrate light scattering. The Hells Canyon region also has a summer b_{ext} peak when light scattering by organics is largest. The b_{ext} in all of the northwestern urban regions peaks in the cold months. Similar to the eastern and southwestern United States, the cold month peaks in b_{ext} were partially due to increased light scattering by ammonium nitrate, as well as increased light scattering by organics at a number of the urban regions. The northwestern urban ammonium sulfate light scattering is unique in that it does not peak in the summer months, and in Boise, Idaho, and Missoula, Montana, ammonium sulfate light scattering actually peaks in the cold months.

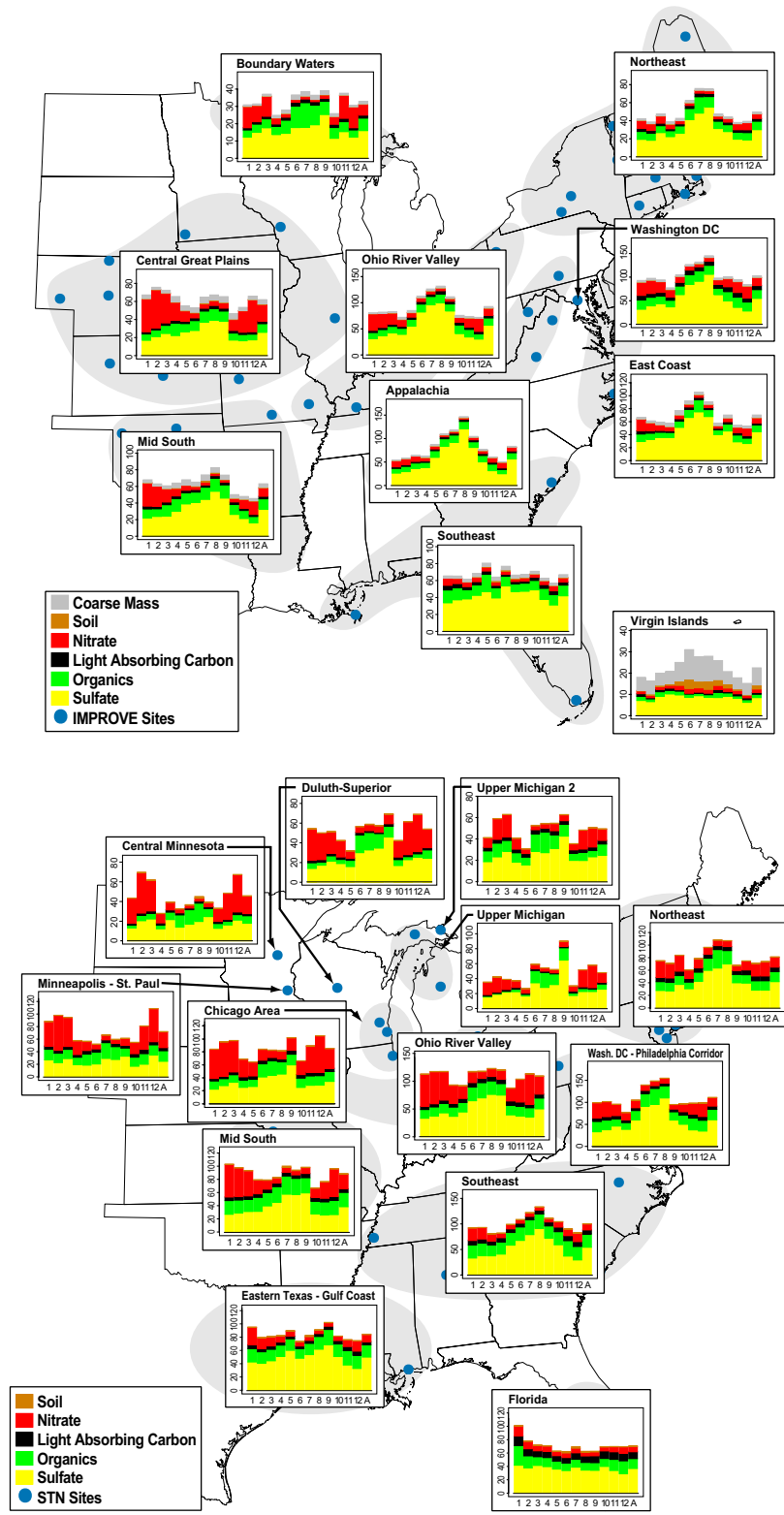


Figure S.13. Monthly particulate contributions to reconstructed b_{ext} (Mm^{-1}) for regions in the eastern United States using IMPROVE data (top) and STN data (bottom). Note, STN does not measure coarse mass.

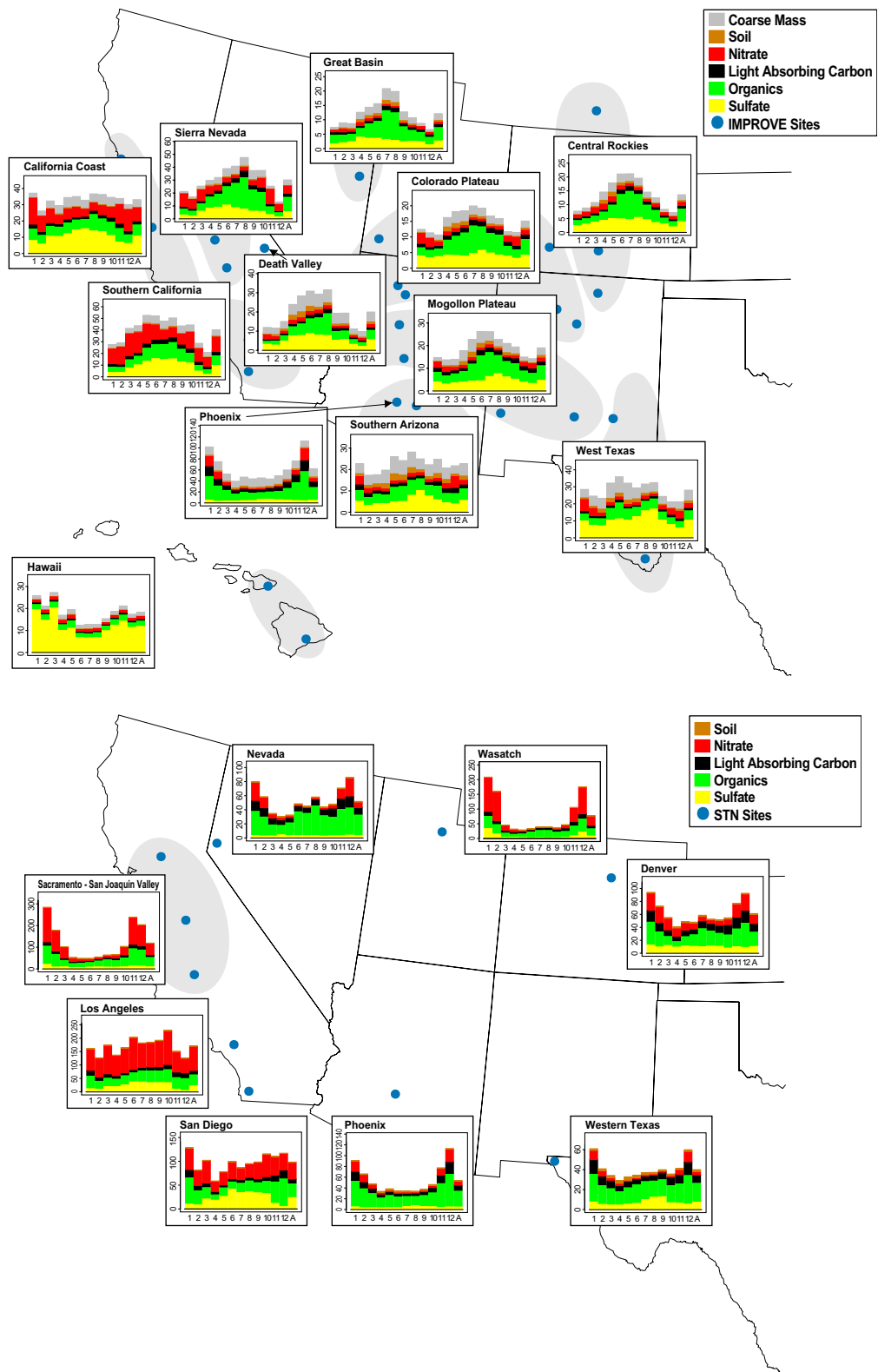


Figure S.14. Monthly particulate contributions to reconstructed b_{ext} (Mm^{-1}) for regions in the southwestern United States using IMPROVE data (top) and STN data (bottom). Note, STN does not measure coarse mass.

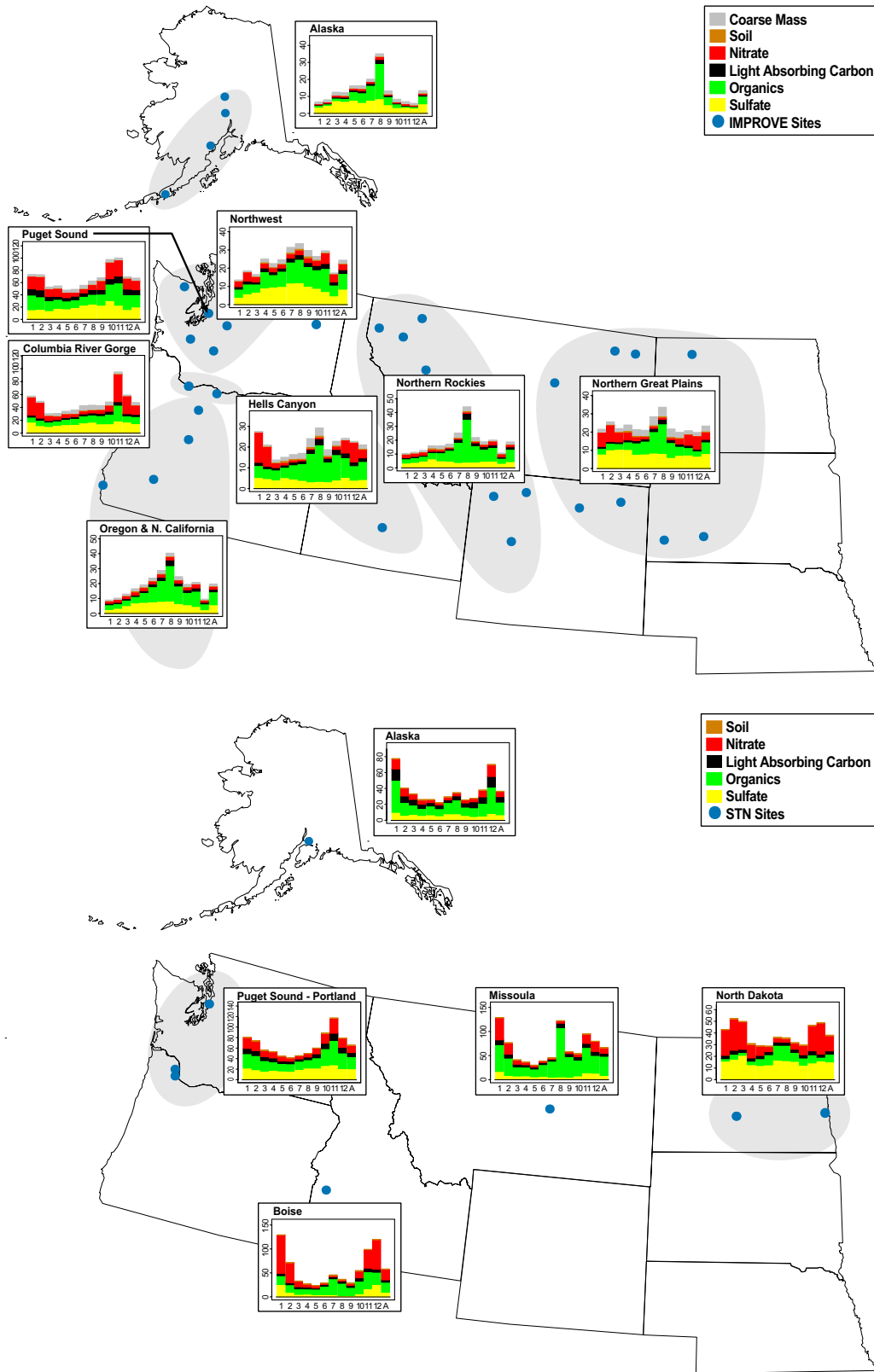


Figure S.15. Monthly particulate contributions to reconstructed b_{ext} (Mm^{-1}) for regions in the northwestern United States using IMPROVE data (top) and STN data (bottom). Note, STN does not measure coarse mass.

S.4 TEMPORAL TRENDS IN FINE AEROSOL SPECIES CONCENTRATIONS AND AEROSOL EXTINCTION

The results of several studies investigating monotonic trends in fine aerosol species concentrations are summarized in this report. Discussions are included on the following topics: the uncertainty in sulfate concentration trends [White et al., 2005], the 10-year spatial and temporal trends in sulfate concentrations and SO₂ emissions [Malm et al., 2002], 10-year trends in visibility [NPS, 2006], >7-year trends in organic and elemental carbon (OC and EC) [Schichtel et al., 2004], and the Visibility Information Exchange Web System (VIEWS) annual summary trends tools.

The effects of sampling and analytical error on time trends derived from routine monitoring were examined in White et al. [2005]. The analysis was based on actual concentration differences observed among three long sulfate series recorded by collocated and independent measurements at Shenandoah National Park. Five-year sulfate trends at this location were shown to include a 1-sigma uncertainty of about 1%/year from measurement error alone. This is significantly more than would be estimated under naive statistical assumptions from the demonstrated precision of the measurements. The excess uncertainty arises from subtle trends in the errors themselves.

Legislative and regulatory mandates have resulted in reduced sulfur dioxide (SO₂) emissions in both the eastern and western United States, with anticipation that concurrent levels of ambient SO₂, SO₄²⁻, and rainwater acidity would decrease. Spatial and temporal trends in ambient SO₄²⁻ concentrations from 1988 to 1999, SO₂ emissions from 1990 to 1999, and the relationship between these two variables were examined in Malm et al. [2002]. The SO₄²⁻ concentration data came from combining data from IMPROVE and the Clean Air Status and Trends Network (CASTNet). In the East, the largest SO₄²⁻ decreases in the 80th percentile concentrations occurred north of the Ohio River valley, while most monitoring sites south of Kentucky and Virginia showed increasing and decreasing trends that were not statistically significant. Big Bend National Park, Texas, Cranberry, North Carolina, and Lassen Volcanic National Park, California, are the only areas that show a statistically significant increase in SO₄²⁻ mass concentrations. The 1990–1999 annual 80th percentile SO₄²⁻ time series were compared to the annual SO₂ emissions over four broad United States regions. Each region had a unique time series pattern, with the SO₄²⁻ concentrations and SO₂ emissions closely tracking each other over the 10-year period. Both the SO₄²⁻ and SO₂ emissions decreased in the Northeast (28%) and the West (15%), while there was little change in the Southeast and a 15% increase over Texas, New Mexico, and Colorado.

Trends in the haze index, measured in deciviews, were examined for the 10-year period 1995–2004 by the National Park Service (http://www2.nature.nps.gov/air/Pubs/pdf/gpra/Gpra2005_Report_03202006_Final.pdf). Trends in the annual average 20% best and worst days were examined using the Theil regression method for the IMPROVE sites with at least 6 complete years out of the 10-year period. Visibility was stable (insignificant trends) or improving at all IMPROVE sites at the 0.05 significance level. Acadia, Moosehorn, Lye Brook, Dolly Sods, and Shenandoah showed statistically significant improving visibility trends for the clearest days at eastern national park monitoring sites. Great Smoky Mountains, Okefenokee, Mammoth Cave, and Washington, D.C., also had improving

trends on the haziest visibility days. Statistically significant improving trends for the clearest visibility days were observed at 17 sites in the western United States including Alaska. Mount Rainier also had an improving trend on the haziest visibility days. No site included in the analysis had a significant worsening trend on either the clearest or haziest visibility days.

Theil regression was used to examine trends in winter and summer elemental and organic carbon at the 54 sites with 7 or more years of data in Schichtel et al. [2004]. Winter EC concentrations decreased significantly at most monitoring sites in the Pacific coastal states and throughout the eastern United States, with median EC concentrations decreasing from 50% to 75% over a 10-year time period. Winter OC concentrations from Washington State to northern California showed similar significant decreases, but Acadia, Maine, was the only monitoring site in the eastern United States with a significant downward trend. Unlike EC, wintertime OC increased at a number of monitoring sites in the southeastern United States, though not significantly. Most sites in the Intermountain West did not show significant winter trends in either EC or OC.

VIEWS is a web-based system that presents data and tools to summarize and display data to aid those who are implementing the Regional Haze Rule enacted in 1999 by the EPA to reduce regional haze and improve visibility in national parks and wilderness areas. As part of this effort, a long-term temporal trends tool was developed that allows a user to quickly create and browse trends of aerosol concentrations and their contribution to light extinction over any monitoring site's sampling period. Various temporal aggregation and smoothing options are available, including the Regional Haze Rule metrics for tracking trends in haze. In addition, a Theil regression analysis can be conducted on each temporal trend.

S.5 IMPROVE DATA QUALITY ASSURANCE

The IMPROVE program's quality assurance system, data validation procedures, and results from a collection of nitrate data quality studies are described in Chapter 5. The first section provides an overview of the IMPROVE network's quality assurance system and the data validation procedures conducted by CIRA (the Cooperative Institute for Research in the Atmosphere). Section 5.2 summarizes the results from a historical data validation review of IMPROVE data collected from 1988 through 2003. Section 5.3 summarizes the results from several studies designed to investigate potential data quality issues related to IMPROVE's nitrate measurements.

S.6 SPECIAL STUDIES ASSOCIATED WITH THE IMPROVE PROGRAM

The results of four special studies conducted in association with the IMPROVE program since the 2000 IMPROVE report are summarized. The Big Bend Regional Aerosol and Visibility Observational (BRAVO) study is summarized in section 6.1. Big Bend National Park is located in southwestern Texas along the Mexican-Texas border. During the 1990s, the haze at Big Bend and other sites in west Texas and southern New Mexico increased, further obscuring Big Bend's and nearby regions' scenic beauty. In response to the increased haze, the BRAVO study was conducted. This was an intensive monitoring study sampling aerosol physical, chemical, and optical properties, as well atmospheric dispersion using synthetic tracers from July through October 1999. The monitoring was followed by a multiyear assessment of the causes of

haze in Big Bend National Park, Texas, with the primary purpose to identify the source regions and source types responsible for the haze at Big Bend.

The Yosemite Aerosol Characterization Study (YACS) is summarized in section 6.2. YACS was an intensive field measurement campaign conducted by a number of U.S. research groups from 15 July to 4 September 2002 at Yosemite National Park, California. The objectives of the study were to determine appropriate values for converting analyzed aerosol carbon mass to ambient aerosol organic carbon mass; develop an improved understanding of the visibility-impairment-related characteristics of a smoke/organic carbon-dominated aerosol, including the role of relative humidity in modifying visibility impairment; and examine the sources contributing to high aerosol organic carbon mass concentrations.

The findings from the review of the IMPROVE equation for estimating ambient light extinction coefficients are summarized in section 6.3. Compliance under the Regional Haze Rule is based on IMPROVE protocols for reconstructing aerosol $PM_{2.5}$ mass concentrations and light extinction coefficients (b_{ext}) from speciated mass concentrations. Hand and Malm (http://vista.cira.colostate.edu/improve/Publications/GrayLit/016_IMPROVEeqReview/IMPROVEeqReview.htm) recently reviewed the assumptions and some associated uncertainties inherent in the IMPROVE formulation for reconstructing light extinction. Refinements were suggested when data exist to support modifications to the assumptions used to derive the IMPROVE equation. However, refinements of several of the assumptions are not possible at this time because existing data do not warrant them or because further measurements are required. The suggested refinements of the IMPROVE equation include

- changing the R_{oc} factor used to compute particulate organic matter from 1.4 to 1.8;
- modifying the $f(RH)$ scattering enhancement curve to reflect some water associated with particles below a relative humidity of 40%;
- including sea salt in reconstructed mass and extinction equations;
- modifying values of dry mass scattering efficiencies to reflect current data and functional relationships between mass scattering efficiency and mass concentration;
- site-specific Rayleigh scattering based on elevation and the annual average temperature of a monitoring site;
- the addition of a NO_2 light absorption term used at sites with available data.

The results of a coarse mass speciation study are included in section 6.4. To more fully investigate the composition of coarse particles, a program of coarse particle sampling and speciation analysis at nine of the IMPROVE sites was initiated 19 March 2003 and operated through the year 2004. The study was motivated by a few short-term special studies at national parks and showed that coarse mass (2.5–10 μm) is not limited to only crustal minerals but can also consist of a substantial amount (≈ 40 –50%) of carbonaceous material and inorganic salts such as calcium nitrate and sodium nitrate. Crustal minerals (soil) were the single largest contributor to coarse mass (CM) at all but one monitoring location. The average fractional contributions ranged from a high of 76% at Grand Canyon National Park to a low of 34% at Mount Rainier National Park. The second largest contributor to CM was organic mass, which on an average annual fractional basis was highest at Mount Rainier at 59%. At Great Smoky

Mountains National Park, organic mass contributed 40% on average, while at four sites organic mass concentrations contributed between 20% and 30% of the CM. Nitrates were on average the third largest contributor to CM concentrations. The highest fractional contributions of nitrates to CM were at Brigantine National Wildlife Refuge, Great Smoky Mountains National Park, and San Gorgonio wilderness area at 10–12%. Sulfates contributed less than about 5% at all sites.

REFERENCES

- Malm, W. C., B. A. Schichtel, R. B. Ames, and K. A. Gebhart (2002), A 10-year spatial and temporal trend of sulfate across the United States, *J. Geophys. Res.*, 107.
- National Park Service (2006), 2005 Annual performance & progress report: Air quality in national parks, available at http://www2.nature.nps.gov/air/Pubs/pdf/gpra/Gpra2005_Report_03202006_Final.pdf.
- Schichtel, B. A., W. C. Malm, and W. H. White (2004), Organic and elemental carbon long-term trends and spatial patterns in rural United States, presented at the Regional and Global Perspectives on Haze: Causes, Consequences and Controversies-Visibility Specialty Conference, Air & Waste Management Association, Asheville, NC, October 25-29.
- White, W. H., L. L. Ashbaugh, N. P. Hyslop, and C. E. Mcdade (2005), Estimating measurement uncertainty in an ambient sulfate trend, *Atmos. Environ.*, 39, 6857-6867.